



# Quantifying land carbon cycle feedbacks under negative CO<sub>2</sub> emissions

V. Rachel Chimuka<sup>1</sup>, Claude-Michel Nzotungicimpaye<sup>1,a</sup> & Kirsten Zickfeld<sup>1</sup>

<sup>1</sup>Department of Geography, Simon Fraser University, Burnaby, BC, V5A 1S6, Canada

5 <sup>a</sup> Now at Department of Geography, Planning and Environment, University of Concordia, Montréal, QC, H3G 1M8, Canada

*Correspondence to:* V. Rachel Chimuka (rchimuka@sfu.ca)

**Abstract.** Land and ocean carbon sinks play a major role in regulating atmospheric CO<sub>2</sub> concentration and climate. However, their future efficiency depends on feedbacks in response to changes in atmospheric CO<sub>2</sub> concentration and climate, namely the concentration-carbon and climate-carbon feedbacks. Since carbon dioxide removal is a key mitigation measure in emission scenarios consistent with global temperature goals in the Paris agreement, understanding carbon cycle feedbacks under negative CO<sub>2</sub> emissions is essential. This study investigates land carbon cycle feedbacks under positive and negative CO<sub>2</sub> emissions using an Earth system model driven with idealized scenarios of atmospheric CO<sub>2</sub> increase and decrease, run in three modes. Our results show that the magnitude of carbon cycle feedbacks differs between the atmospheric CO<sub>2</sub> ramp-up (positive emissions) and ramp-down (negative emissions) phases. These differences are likely largely due to climate system inertia: the response in the ramp-down phase represents the response to both the prior positive emissions and negative emissions. To isolate carbon cycle feedbacks under negative emissions and quantify these feedbacks more accurately, we propose a novel approach that uses zero emissions simulations to reduce this inertia. We find that the magnitudes of the concentration-carbon and climate-carbon feedbacks under negative emissions are larger in our novel approach than in the standard approach. This has two implications: using feedback parameters from the standard approach will (1) underestimate carbon release under negative emissions due to the concentration-carbon feedback, and (2) underestimate carbon gain due to the climate-carbon feedback. Given that the concentration-carbon feedback is the dominant feedback, quantifying carbon cycle feedbacks with the standard approach will result in the underestimation of carbon loss under negative emissions, thereby overestimating the effectiveness of negative emissions in drawing down CO<sub>2</sub>.

25

30



## 1 Introduction

Anthropogenic CO<sub>2</sub> emissions have increased substantially since the preindustrial era, increasing the risk of “severe, pervasive and irreversible impacts” to the Earth system (IPCC, 2022). In an effort to reduce greenhouse gas emissions, nations adopted the Paris Agreement, which stipulated that surface warming should be kept well below 2°C above preindustrial levels and encouraged efforts to further limit it to 1.5°C (UNFCCC, 2015). Carbon dioxide removal (CDR) is a key mitigation measure in emission scenarios that are consistent with these climate goals (Ciais et al., 2013; Fuss et al., 2014; Rogelj et al., 2018; Rogelj et al., 2019; IPCC, 2022).

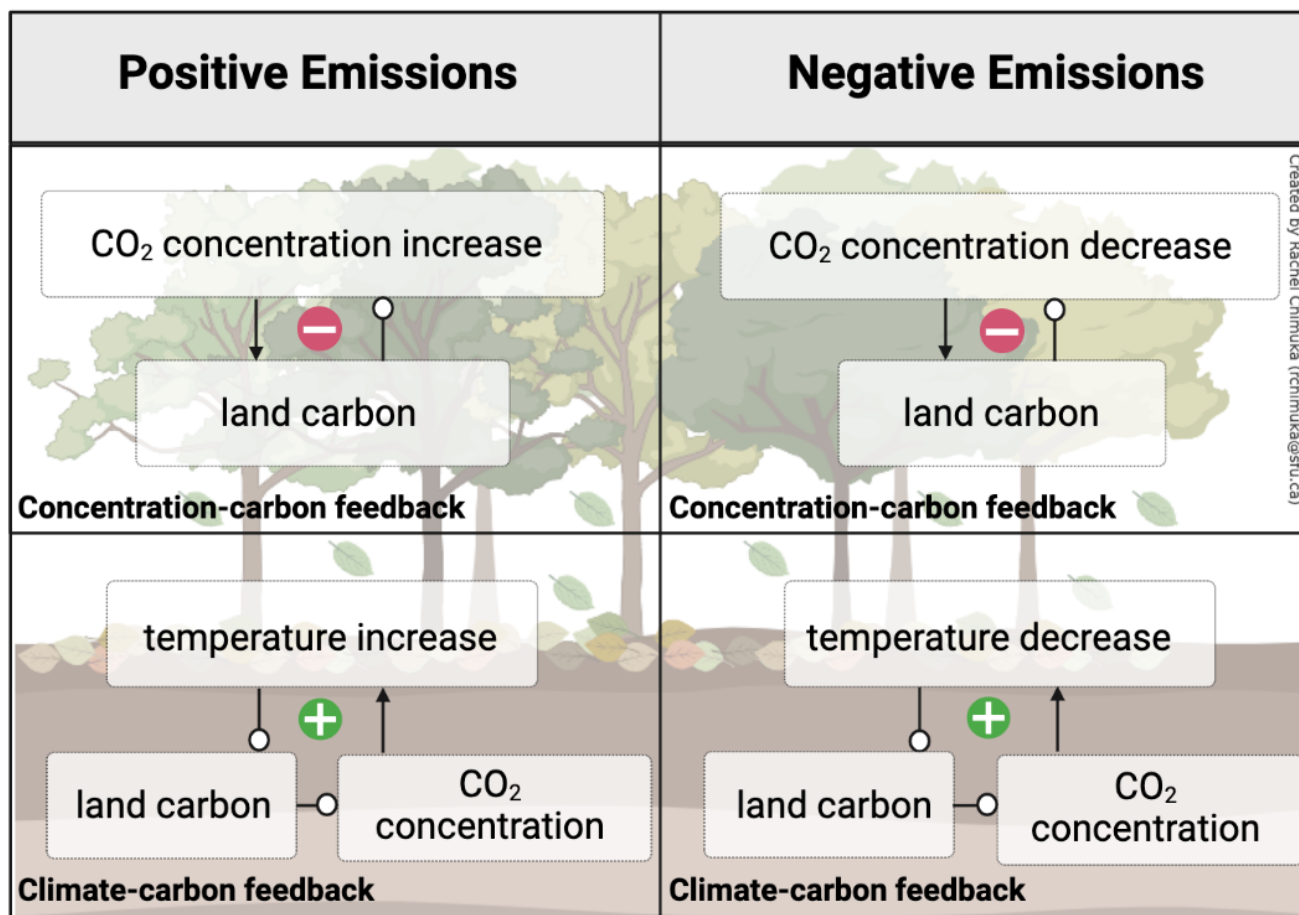
The land and ocean carbon sinks play a major role in regulating atmospheric CO<sub>2</sub> concentration by absorbing approximately half of current anthropogenic CO<sub>2</sub> emissions (Friedlingstein et al., 2021). However, this rate of absorption is sensitive to changes in climate and atmospheric CO<sub>2</sub> concentration (Cox et al., 2000; Boer & Arora, 2010; Arora et al., 2013; Boer & Arora, 2013; Arora et al., 2020). As atmospheric CO<sub>2</sub> concentration increases, carbon sinks will take up more carbon through air-sea exchange and CO<sub>2</sub> fertilization, resulting in a negative concentration-carbon cycle feedback (Boer & Arora, 2010; Arora et al., 2013; Schwinger & Tjiputra, 2018). Conversely, changing climate, in response to the increasing CO<sub>2</sub> concentration, will decrease the ability of carbon sinks to take up carbon, resulting in a positive climate-carbon cycle feedback (Cox et al., 2000; Jones et al., 2003; Fung et al., 2005; Friedlingstein et al., 2006; Boer & Arora, 2010; Zickfeld et al., 2011; Boer & Arora, 2013; Friedlingstein et al., 2014; Schwinger & Tjiputra, 2018).

Since the dominant feedback controlling land and ocean carbon uptake is the negative concentration-carbon feedback, the land and ocean are currently carbon sinks (Arora et al., 2020). However, these sinks are expected to weaken or even reverse under net-negative CO<sub>2</sub> emissions, that is, when the amount of CO<sub>2</sub> removed from the atmosphere exceeds the amount of CO<sub>2</sub> added to the atmosphere (Cao & Caldeira, 2010; Tokarska & Zickfeld, 2015; Jones et al., 2016). Decreasing CO<sub>2</sub> levels will weaken the CO<sub>2</sub> fertilization effect, decreasing net primary productivity (NPP) more than soil respiration, resulting in a flux of carbon into the atmosphere (Cao & Caldeira, 2010; Tokarska & Zickfeld, 2015). Furthermore, the gradient in the partial pressure of CO<sub>2</sub> at the atmosphere-ocean interface will weaken and eventually reverse, resulting in the outgassing of CO<sub>2</sub> (Cao & Caldeira, 2010; Tokarska & Zickfeld, 2015). Carbon losses from the land and ocean following CDR are expected to significantly decrease the effectiveness of CDR in drawing down atmospheric CO<sub>2</sub> (Tokarska & Zickfeld, 2015; Jones et al., 2016; Zickfeld et al., 2021).

The behaviour of land carbon cycle feedbacks under positive and negative emissions is shown qualitatively in Figure 1. The dominant concentration-carbon feedback is shown in the top two panels. As the atmospheric CO<sub>2</sub> concentration increases



under positive emissions, the land sequesters more carbon, reducing the atmospheric CO<sub>2</sub> concentration (Boer & Arora, 2010; Arora et al., 2013). However, under negative emissions, the declining atmospheric CO<sub>2</sub> concentration weakens and eventually reverses the land carbon sink, returning CO<sub>2</sub> to the atmosphere. This feedback is negative because it promotes carbon sequestration under positive emissions and drives carbon loss under negative emissions. The bottom two panels show the behaviour of the less dominant climate-carbon feedback. As the climate warms under positive emissions, the land loses carbon to the atmosphere, increasing the atmospheric CO<sub>2</sub> and causing further warming (Cox et al., 2000; Jones et al., 2003; Fung et al., 2005; Friedlingstein et al., 2006; Boer & Arora, 2010; Zickfeld et al., 2011; Boer & Arora, 2013; Friedlingstein et al., 2014). With cooling, the land carbon source weakens and eventually turns into a carbon sink, sequestering carbon and further cooling the climate under negative emissions. This positive feedback acts to amplify warming (cooling) under positive (negative) emissions.



75 **Figure 1: Carbon cycle feedback schematic illustrating the behaviour of the negative concentration-carbon feedback and positive climate-carbon feedback under positive and negative emissions. Each feedback loop under positive (negative) emissions starts with an increase (decrease) in atmospheric CO<sub>2</sub> concentration or surface air temperature. Arrows indicate a positive coupling (change in the same direction) between components and lines with empty circles indicate a negative coupling (change in the opposite direction) between components.**

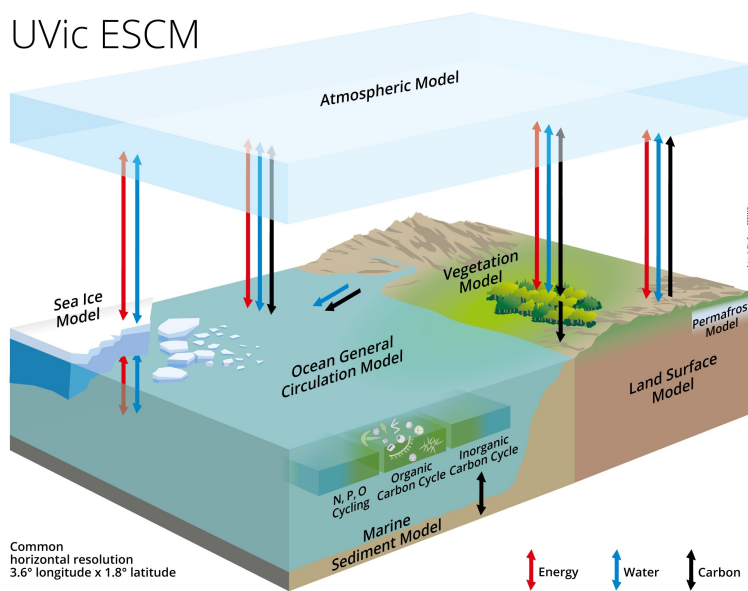


80 The goal of this study is to quantify land carbon cycle feedbacks under negative emissions. We address two research questions:  
(1) How does the magnitude of carbon cycle feedbacks under negative emissions compare to that under positive emissions?  
(2) Is the approach currently used to quantify carbon cycle feedbacks under positive emissions adequate to quantify feedbacks  
85 under negative emissions? If not, how can this approach be improved upon? This study investigates carbon cycle feedbacks  
under positive and negative emissions in an Earth system model driven with an idealized scenario with a 1% per year increase  
and decrease in atmospheric CO<sub>2</sub> concentration. Our study complements the only existing study on ocean carbon cycle  
feedbacks under negative emissions (Schwinger & Tjiputra, 2018) by exploring the behaviour of these feedbacks on land. We  
propose a novel approach to quantifying carbon cycle feedbacks under negative emissions and provides insight into the role  
of these feedbacks in determining the effectiveness of carbon dioxide removal in reducing CO<sub>2</sub> levels.

## 2 Methodology

### 90 2.1 Model Description

The University of Victoria Earth System Climate Model (UVic ESCM, version 2.10) (**figure 2**) is a model of intermediate  
complexity with a horizontal grid resolution of 1.8° (meridional) x 3.6° (zonal) (Weaver et al., 2001; Mengis et al., 2020). The  
model consists of a simplified atmospheric model, a 3D ocean general circulation model, including ocean inorganic and organic  
carbon cycle models, coupled to a dynamic-thermodynamic sea ice model, and a land surface model coupled to a vegetation  
95 model (including permafrost) (Mengis et al., 2020). The atmosphere is a 2D energy-moisture balance model with dynamical  
wind feedbacks. Atmospheric heat and freshwater are transported through diffusion and advection (Weaver et al., 2001), based  
on wind velocities prescribed from monthly climatological wind fields from NCAR/NCEP reanalysis data (Eby et al., 2013).  
The 19-layer 3D ocean general circulation model is based on the Geophysical Fluid Dynamics Laboratory (GFDL) Modular  
Ocean Model Version 2 (MOM2) (Pacanowski, 1995). The coupled dynamic-thermodynamic sea ice model simulates sea ice  
100 dynamics through elastic, viscous and plastic deformation and flow mechanisms (Weaver et al., 2001). Ocean carbon is  
represented by an inorganic ocean carbon model following the Ocean Carbon Model Intercomparison Protocol (OCMIP), and  
a NPZD (nutrient, phytoplankton, zooplankton, detritus) model of ocean biology simulating carbon uptake by the biological  
pump, accounting for phytoplankton light and iron limitations (Keller et al., 2012). The land surface model, based on the  
Hadley Centre Met Office Surface Exchange Scheme (MOSES), simulates the terrestrial carbon cycle and is coupled to the  
105 Top-Down Representation of Interactive Foliage and Flora including Dynamics (TRIFFID) model which simulates vegetation  
and soil carbon (Meissner et al., 2003). This model version also includes a permafrost carbon model in the soil module that  
generates permafrost through a diffusion-based scheme (MacDougall & Knutti, 2016).



110 **Figure 2: University of Victoria Earth System Climate Model (UVic ESCM) Schematic. Energy, water and carbon exchanges between model components are represented by arrows. Figure reproduced with permission from Mengis et al. (2020).**

## 2.2 Model Simulations

We performed a preindustrial spin-up simulation to equilibrate the model with the preindustrial CO<sub>2</sub> concentration (~285ppm). All other greenhouse gas concentrations, surface land conditions and orbital parameters were held at 1850 levels according to the Coupled Model Intercomparison Project Phase 6 (CMIP6) experimental design protocol (Eyring et al., 2016). The solar forcing was set to the 1850 – 1873 mean and the volcanic forcing was held at its average over 1850 – 2014, also consistent with CMIP6 protocol (Eyring et al., 2016).

To explore how the magnitude of carbon cycle feedbacks under positive emissions differs from that under negative emissions, we ran the “CDR-reversibility” simulation from the Carbon Dioxide Removal Model Intercomparison Project (CDRMIP) (Keller et al., 2018). Starting from a preindustrial equilibrium state, atmospheric CO<sub>2</sub> concentration was prescribed to increase at 1% per year until quadrupling, then decline back to preindustrial levels at the same rate. We refer to the section of the prescribed CO<sub>2</sub> concentration trajectory with increasing (decreasing) CO<sub>2</sub> concentration as the ramp-up (ramp-down) phase.

125 We also ran a zero emissions simulation (“Zeroemit”) for use in our novel approach for quantifying carbon cycle feedbacks under negative emissions. This simulation was initialized from the peak atmospheric CO<sub>2</sub> concentration in the “CDR-reversibility” simulation and run in emissions-driven configuration. Emissions were set to zero at the start of the simulation, then CO<sub>2</sub> was allowed to evolve.



130 The “CDR-reversibility” and “Zeroemit” simulations were run in three modes, following the C4MIP protocol for the quantification of carbon cycle feedbacks (Friedlingstein et al., 2006; Arora et al., 2013; Jones et al., 2016; Arora et al., 2020):

1. Fully coupled mode (FULL): the land and ocean carbon sinks are subject to changing atmospheric CO<sub>2</sub> concentration and climate.
2. Biogeochemically coupled mode (BGC): the land and ocean carbon sinks are subject to changing CO<sub>2</sub> concentration alone. The radiation module uses preindustrial CO<sub>2</sub> levels.
- 135 3. Radiatively coupled mode (RAD): the land and ocean carbon sinks are subject to changes in climate alone.

### 2.3 Approaches to Feedback Quantification

In our first approach (referred to as the “standard” approach), we use the “CDR-reversibility” simulation to quantify carbon cycle feedbacks under positive and negative emissions. Although this simulation is highly idealized, the ramp-up phase is standardly used to investigate carbon cycle feedbacks under positive emissions, and therefore, allows easier comparison of these results to other literature. The ramp-up phase represents the response to positive emissions alone. However, the ramp-down phase represents the response to both the prior positive emissions and negative emissions because negative emissions are applied from a transient (that is, time-evolving) state (Zickfeld et al., 2016; Keller et al., 2018). As a result, carbon cycle feedbacks quantified from the ramp-down phase do not represent the response to negative emissions alone.

145 Our second and novel approach, therefore, aims to improve the quantification of carbon cycle feedbacks under negative emissions in an experimental design utilizing both the “CDR-reversibility” and “Zeroemit” simulations. Since the “Zeroemit” simulation quantifies the “committed” response to the prior positive emissions, this simulation was subtracted from the ramp-down phase of the “CDR-reversibility” simulation to isolate the response to negative emissions alone. A similar approach was used in Zickfeld et al. (2016). From our approach – referred to as the “Ramp-down – Zeroemit” approach – we also quantify carbon cycle feedbacks for comparison to feedbacks from the first approach. The main assumption made here is that of linearity, that is, we assume that the committed carbon cycle response to past positive emissions and the carbon cycle response to negative emissions combine linearly to the total carbon cycle response in the ramp-down phase.

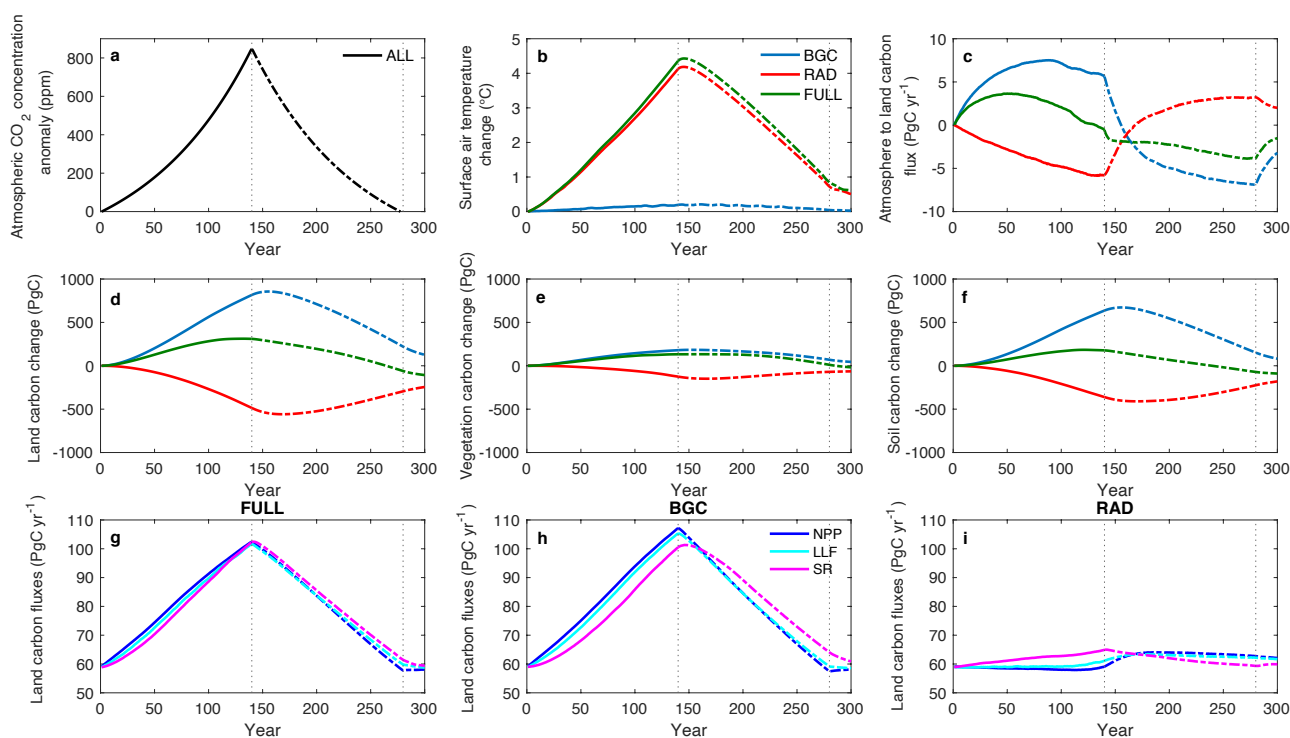
We use integrated flux-based feedback parameters from Friedlingstein et al. 2006 to quantify carbon cycle feedbacks in both approaches, under both positive and negative emissions (**see supplementary material**). The BGC and RAD modes are used to isolate the system response to changes in atmospheric CO<sub>2</sub> concentration and climate, respectively, allowing for the quantification of the concentration-carbon and climate-carbon feedbacks. Climate-carbon feedbacks can also be quantified from the difference between the FULL and BGC modes (Arora et al., 2020; **see supplementary equations 3.7 and 3.8**). The resulting feedback parameters differ from those quantified from the BGC mode alone due to nonlinearities in carbon cycle feedbacks (Zickfeld et al., 2011).



### 3 Results

#### 3.1 “CDR-reversibility” Carbon Cycle Feedback Analysis

Our results focus on the ramp-down phase of the “CDR-reversibility” simulation and compare the system response in this phase to that in the ramp-up phase. While the prescribed atmospheric CO<sub>2</sub> concentration for the “CDR-reversibility” simulations is the same, the temperature response differs by mode (**figure 3(a, b)**). In the FULL and RAD modes, surface air temperature increases approximately linearly with increasing atmospheric CO<sub>2</sub> concentration, continues to increase for approximately half a decade after atmospheric CO<sub>2</sub> concentration peaks, then decreases with decreasing CO<sub>2</sub> concentration. Surface air temperature declines more slowly in the ramp-down phase due to the thermal inertia of the ocean, and therefore, does not return to preindustrial levels by the end of the ramp-down phase. The temperature response in the FULL mode is consistent with earlier studies (Boucher et al., 2012; Zickfeld et al., 2016; Park & Kug, 2021). Surface air temperature in the BGC mode changes only marginally: surface air temperature increases slightly with increasing CO<sub>2</sub> concentration and decreases as the CO<sub>2</sub> concentration decreases. This temperature change is driven by biophysical responses to changing atmospheric CO<sub>2</sub>. Biophysical effects are also responsible for the difference in warming between the FULL and RAD modes (Arora et al., 2020). The temperature response in the ramp-up phase of the FULL, BGC and RAD modes is consistent with Arora et al. (2020) while the temperature response in the ramp-up and ramp-down phases of all three modes is consistent with Schwinger & Tjiputra (2018).







180 **Figure 3: a. Prescribed atmospheric CO<sub>2</sub> concentration b. surface air temperature change c. atmosphere to land carbon flux and d. land e. vegetation and f. soil carbon changes in the fully coupled (FULL), biogeochemically coupled (BGC) and radiatively coupled (RAD) “CDR-reversibility” simulations. Panels a, b, and d - f are calculated relative to 1850 (preindustrial). Carbon fluxes for the three modes are shown in the bottom panels (g, h, i). NPP = net primary productivity, LLF = leaf litter flux and SR = soil respiration. Solid lines represent the ramp-up phase and dot-dashed lines represent the ramp-down phase. The vertical dotted lines mark the beginning and end of the ramp-down phase.**

### 3.1.1 Land Carbon Change in the FULL Mode

185 **Figure 3(d)** shows land carbon changes as a function of time. In the FULL mode, the land gains carbon at a decreasing rate, then begins to slowly lose carbon 7 years before the peak atmospheric CO<sub>2</sub> concentration is reached. Similar carbon uptake and loss patterns are observed for the soil carbon pool, which starts losing carbon roughly 20 years before the peak in atmospheric CO<sub>2</sub> concentration, but vegetation carbon loss begins 2 years after the peak atmospheric CO<sub>2</sub> concentration (**figure 3(e, f)**). Our results differ from the earlier studies (MacDougall, 2019; Arora et al., 2020) wherein the land carbon pool remains  
190 a carbon sink in the ramp-up phase. MacDougall (2019) shows that the soil carbon sink switches into a source later in the ramp-up phase than our results show. Furthermore, other studies (Boucher et al., 2012; Zickfeld et al., 2016) show that both vegetation and soil carbon sinks persist throughout the ramp-up phase. The land loses carbon throughout the ramp-down phase (**figure 3(d)**). Earlier studies show continued land carbon uptake in the early ramp-down phase followed by land carbon loss (Boucher et al., 2012; Zickfeld et al., 2016; Park & Kug, 2021). Changes in land carbon are governed by the balance between  
195 net primary productivity (NPP) and soil respiration. Carbon gain is driven by the CO<sub>2</sub> fertilization effect: photosynthesis is enhanced under increasing CO<sub>2</sub> concentration, increasing NPP (**figure 3(g)**) (Arora et al. 2013). Soil respiration also increases with warming (**figure 3(g)**). Initially, soil respiration remains below NPP, but the rate of increase of NPP declines faster and soil respiration exceeds NPP towards the end of the ramp-up phase. This occurs due to the different response timescales of NPP and soil respiration: NPP depends on atmospheric CO<sub>2</sub> changes, whereas soil respiration depends on temperature change,  
200 which lags behind the change in CO<sub>2</sub> concentration (Cao & Caldeira, 2010). In the ramp-down phase, NPP decreases as the CO<sub>2</sub> fertilization effect weakens, whereas soil respiration continues to increase for a year before decreasing at a slower rate than NPP, driven by decreasing surface air temperature and soil carbon.

### 3.1.2 Land Carbon Change in the BGC Mode

In the BGC mode, the land sequesters carbon in the ramp-up phase, remains a carbon sink until 16 years after the peak in CO<sub>2</sub>  
205 concentration, then switches into a source of carbon (**figure 3(d)**). A similar lag is observed for both vegetation and soil carbon pools, but the soil carbon sink persists for five years longer than the vegetation carbon sink (**figure 3(e, f)**). The land sequesters carbon in the ramp-up phase due to the CO<sub>2</sub> fertilization effect, which increases NPP (**figure 3(h)**) (Arora et al. 2013). In the UVic ESCM, soil respiration depends on soil temperature, moisture, and carbon content (Cox et al., 2001; Mengis et al., 2020). Since changes in surface air temperature in the BGC mode are small (**figure 3(b)**), changes in the first two factors are negligible  
210 and soil carbon content is the main driver of soil respiration changes. Soil respiration increases with increasing soil carbon, but NPP remains higher, resulting in land carbon uptake in the ramp-up phase (**figure 3(h)**). In the ramp-down phase, NPP





decreases as the CO<sub>2</sub> fertilization effect weakens, whereas soil respiration continues to increase before decreasing at a slower rate than NPP, following changes in soil carbon (**figure 3(h)**). NPP declines below soil respiration, and the land switches into a carbon source.

### 215 3.1.3 Land Carbon Change in the RAD Mode

The land loses carbon in the ramp-up phase of the RAD mode, remains a carbon source until roughly 30 years after the peak in atmospheric CO<sub>2</sub> concentration, then switches into a carbon sink (**figure 3(d)**). Both vegetation and soil carbon pools exhibit a similar lag, but the vegetation carbon pool remains a carbon source for a decade longer than the soil carbon pool (**figure 3(e, f)**). The land loses carbon in the ramp-up phase because NPP decreases as plant respiration rates increase (**see figure S1**),  
220 whereas soil respiration increases with warming (**figure 3(i)**) consistent with earlier literature (Arora et al., 2020). NPP later increases due to vegetation shifts that occur on decadal to centennial timescales (**see figure S2**) but remains lower than soil respiration. In the ramp-down phase, NPP increases (**figure 3(i)**) as gross primary productivity increases and plant respiration decreases with cooling, then later declines as gross primary productivity declines, because cooler temperatures negatively impact vegetation growth in the high latitudes (**see figures S1, S3**). Soil respiration decreases steadily with declining surface  
225 air temperature, and after a few decades, declines below NPP, and the land switches into a carbon sink.

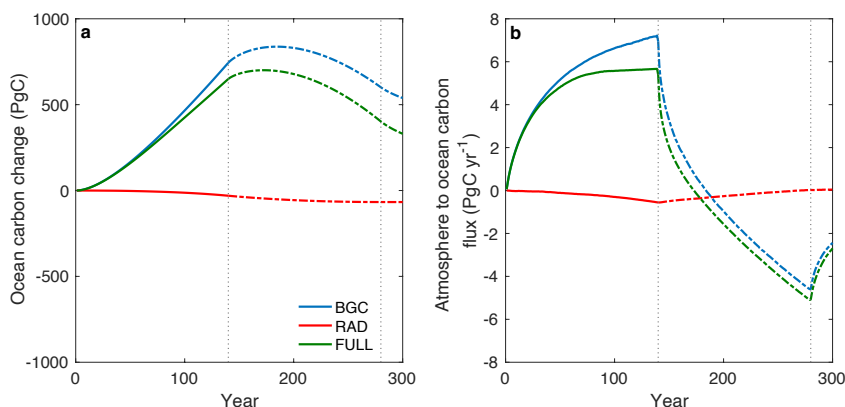
### 3.1.4 Ocean Carbon Change in the FULL, BGC and RAD Modes

In the FULL mode, the ocean gains carbon at a steady rate, then begins to slowly lose carbon roughly three decades after the peak in atmospheric CO<sub>2</sub> concentration (**figure 4(a)**). In the ramp-up phase, the partial pressure of CO<sub>2</sub> in the atmosphere increases, strengthening the partial pressure gradient and driving an influx of CO<sub>2</sub> into the ocean (**figure 4(b)**). In the ramp-  
230 down phase, the gradient in partial pressure weakens and eventually reverses, and the ocean carbon sinks switches into a source. Earlier studies forced with the “CDR-reversibility” simulation also show ocean carbon uptake in the ramp-up phase (MacDougall, 2019; Arora et al., 2020) followed by delayed carbon loss in the ramp-down phase (Boucher et al., 2012; Zickfeld et al., 2016).

235 The ocean exhibits a delayed response in the ramp-down phase of the BGC and RAD modes consistent with Schwinger & Tjiputra (2018). In the BGC mode, the ocean takes up carbon in the ramp-up phase, remains a carbon sink for approximately half a century after the peak atmospheric CO<sub>2</sub> concentration, then switches into a source of carbon (**figure 4(a)**). The partial pressure gradient of CO<sub>2</sub> strengthens in the ramp-up phase, driving CO<sub>2</sub> uptake, then weakens and reverses in the ramp-down phase, promoting carbon loss, but the magnitude of the flux is larger than in the FULL mode (**figure 4(b)**). In the RAD mode,  
240 the ocean loses carbon in the ramp-up phase, remains a carbon source for over a century in the ramp-down phase, then switches into a weak carbon sink (**figure 4(a)**). The ocean outgasses in the ramp-up phase possibly due to climate effects on ocean circulation and the solubility pump (Cox et al., 2000; Fung et al., 2005; Friedlingstein et al., 2006; Zickfeld et al., 2011). In the ramp-down phase, the ocean remains a carbon source for over a century before switching into a weak carbon sink. Ocean



carbon changes in the BGC and RAD modes are also driven by the concentration-carbon and climate-carbon feedbacks. An  
245 in-depth discussion of the mechanisms behind the ocean carbon response is beyond the scope of this paper.



250 **Figure 4: a. Ocean carbon change and b. atmosphere to ocean carbon flux in the fully coupled (FULL), biogeochemically coupled (BGC) and radiatively coupled (RAD) “CDR-reversibility” simulations. Ocean carbon change is calculated relative to 1850 (preindustrial). Solid lines represent the ramp-up phase and dot-dashed lines represent the ramp-down phase. The vertical dotted lines mark the beginning and end of the ramp-down phase.**

### 3.1.5 Sensitivity of Land and Ocean Carbon Pools

To assess the sensitivity of land and ocean carbon pools to changes in atmospheric CO<sub>2</sub> and temperature, we plot carbon changes in the BGC mode as a function of atmospheric CO<sub>2</sub> concentration (**figure 5**) and carbon changes in the RAD mode as a function of surface air temperature (**figure 6**). The trajectory of carbon change differs in the ramp-up and ramp-down phases  
255 of the BGC mode (**figure 5**), a behavior referred to as hysteresis. Hysteresis in the land carbon pool is primarily driven by the soil carbon pool, although the contribution from the vegetation carbon pool is also significant (**figure 5(a, c, d)**). The width of the hysteresis – measured as the vertical distance between the ramp-up and ramp-down trajectories – initially increases, then decreases (**figure 5(a - d)**), except in the vegetation carbon pool where the width of the hysteresis increases throughout the simulation (**figure 5(c)**). The land and ocean carbon pools in the RAD mode also exhibit hysteresis (**figure 6**). The hysteresis  
260 in the land carbon pool is dominated by the soil carbon pool (**figure 5(d)**), and the width of the hysteresis appears to increase throughout the simulation for all carbon pools except the vegetation carbon, which shows nearly constant hysteresis. The observed hysteresis in the land and ocean carbon pools in the BGC and RAD modes is likely largely due to climate system inertia: the carbon cycle response under negative emissions, that is, in the ramp-down phase, is a combination of the response to both negative emissions and the prior positive emissions.

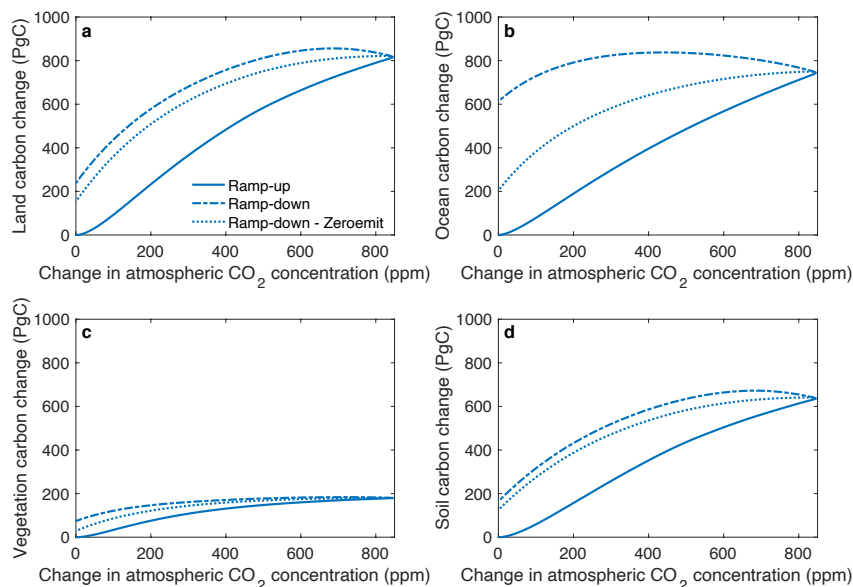
265

Despite the restoration of preindustrial atmospheric CO<sub>2</sub> levels in the BGC mode, the land and ocean carbon pools do not return to their preindustrial states. At the end of the ramp-down phase, the land carbon pool holds approximately 250 PgC more than at preindustrial, with 80 PgC remaining in vegetation and 170 PgC remaining in the soil (**figure 5(a, c, d)**), whereas the ocean carbon pool holds much more carbon (615PgC) than at preindustrial (**figure 5(b)**). In the RAD mode, the land and

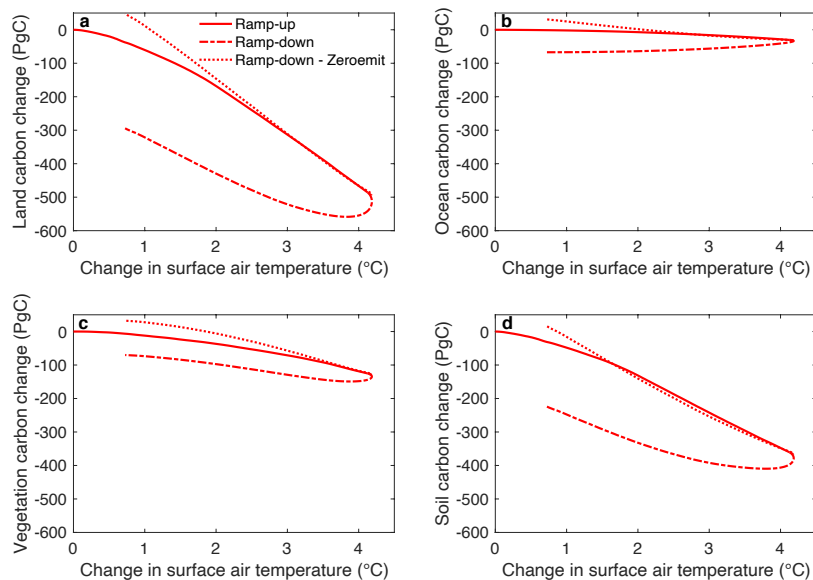


270 ocean carbon lost in the ramp-up phase is not completely regained in the ramp-down phase, though this response would not be  
expected given the asymmetric surface air temperature response in this mode. By the end of the RAD mode, the land carbon  
pool holds approximately 300 PgC less than at preindustrial, with the vegetation carbon pool accounting for 70 PgC and the  
soil carbon pool accounting for the remaining 230PgC (**figure 6(a, b, c)**). The ocean holds only 70PgC less than at  
preindustrial, but unlike the land carbon pool, a miniscule amount of ocean carbon is regained in the ramp-down phase (**figure**  
275 **5(d)**).

Previous studies have shown carbon cycle hysteresis in the FULL mode of the “CDR-reversibility” simulation (Boucher et al.,  
2012; Zickfeld et al., 2016; Park & Kug, 2021), consistent with our results (see **figure S4**). However, in these studies, the  
vegetation and soil carbon pools do not return to their preindustrial states by the end of the ramp-down phase. Our results for  
280 the FULL mode of the “CDR-reversibility” simulation show that the vegetation and soil carbon pools are very close to their  
preindustrial states by the end of the ramp-down phase, consistent with Ziehn et al. (2020), who show a near-return to the  
preindustrial state in the vegetation carbon pool.



285 **Figure 5: a. Land b. ocean c. vegetation and d. soil carbon pool changes as a function of atmospheric CO<sub>2</sub> concentration, taken from the biogeochemically coupled (BGC) “CDR-reversibility” simulation ramp-up and ramp-down phases, and “ramp-down – zeroemit” simulation. All values are calculated relative to 1850 (preindustrial).**



290 **Figure 6: a. Land b. ocean c. vegetation and d. soil carbon pool changes as a function of surface air temperature change, taken from the radiatively coupled (RAD) “CDR-reversibility” simulation ramp-up and ramp-down phases, and “ramp-down – zeroemit” simulation. All values are calculated relative to 1850 (preindustrial).**

### 3.1.6 Carbon Cycle Feedback Parameters quantified from “CDR-reversibility” simulations

300 **Table 1** shows the carbon cycle feedback parameters quantified from the Friedlingstein et al. (2006) carbon cycle feedback framework (see **supplementary material**). The concentration-carbon feedback parameter ( $\beta$ ), which quantifies the concentration-carbon feedback, is computed as the change in land or ocean carbon per unit change in atmospheric CO<sub>2</sub> concentration in the BGC mode. The climate-carbon feedback parameter ( $\gamma$ ) quantifies the climate-carbon feedback as the change in land or ocean carbon per unit change in surface air temperature in the RAD mode (referred to as the RAD approach).  
295 An alternative approach to quantifying the climate-carbon feedback involves taking the difference between the fully coupled and biogeochemically coupled simulations and computing the change in land or ocean carbon per unit change in surface air temperature from that difference (referred to here as the FULL-BGC approach).

300 Feedback parameters are quantified for both the ramp-up and the ramp-down phases i.e., under positive and negative emissions. Feedback parameters under positive emissions are computed at the peak atmospheric CO<sub>2</sub> concentration (quadruple the preindustrial level) using changes in carbon pools, atmospheric CO<sub>2</sub> concentration and surface air temperature computed relative to preindustrial levels. Feedbacks under negative emissions are computed at the return to preindustrial levels (end of  
305 ramp-down phase) using changes in carbon pools, atmospheric CO<sub>2</sub> concentration and surface air temperature computed relative to the time of peak atmospheric CO<sub>2</sub>.



For positive emissions, feedback parameters are positive (negative) for a gain (loss) of carbon. Under negative emissions, both atmospheric CO<sub>2</sub> concentration and surface air temperature decline, resulting in a negative denominator (see supplementary equations 3.3 – 3.6). Therefore, the sign convention is reversed: feedback parameters are negative for a gain in carbon (positive numerator divided by negative denominator) and positive for a loss in carbon (negative numerator divided by negative denominator). The concentration-carbon and climate-carbon feedback parameters shown here can also be derived from figures 5 and 6 respectively by taking the slope of the land or ocean response at the same time points.

In the “CDR-reversibility” simulation, the magnitudes of  $\beta$  and  $\gamma$  for both land and ocean are smaller under negative emissions than under positive emissions (Table 1). Climate-carbon feedback parameters calculated using the FULL-BGC approach (shown in parentheses) are consistent in sign with those calculated using the RAD approach, but the magnitudes of these feedback parameters are larger (see Figure S5 for hysteresis figures for this approach). Carbon cycle feedback parameters are smaller under negative emissions because carbon loss (gain) due to the concentration-carbon (climate-carbon) feedback is reduced due to continued carbon uptake (loss) at the beginning of the ramp-down phase related to carbon cycle inertia. In fact, the ocean continues to lose carbon throughout the ramp-down phase due to the climate-carbon feedback (shown by the positive ocean climate-carbon feedback parameter under negative emissions). As a result, feedback parameters under negative emissions are underestimated, and improving this quantification could be achieved by quantifying and removing this inertia.

Simulations(s) used for calculation of feedback parameters	Positive Emissions				Negative Emissions			
	$\beta_L$	$\beta_O$	$\gamma_L$	$\gamma_O$	$\beta_L$	$\beta_O$	$\gamma_L$	$\gamma_O$
	$(PgC\ ppm^{-1})$		$(PgC\ ^\circ C^{-1})$		$(PgC\ ppm^{-1})$		$(PgC\ ^\circ C^{-1})$	
“CDR-reversibility” simulation taken at 4xCO <sub>2</sub> for positive emissions and at return to preindustrial for negative emissions	0.96	0.88	-117.8 (-121.5)	-7.36 (-22.7)	0.68	0.16	-56.4 (-67)	10.8 (31.1)
“Ramp-up – Zeroemit” simulation taken at 4xCO <sub>2</sub> for positive emissions and at return to preindustrial for negative emissions	0.96	0.88	-117.8	-7.36	0.80	0.84	-157.1	-18.1

325

**Table 1: Carbon cycle feedback parameters under positive and negative emissions. Feedback parameters for negative emissions are positive (negative) for a loss (gain) in carbon. Values shown in parentheses were calculated using the FULL-BGC method: an alternative method for quantifying climate-carbon feedbacks (see supplementary equations 3.7 and 3.8).**

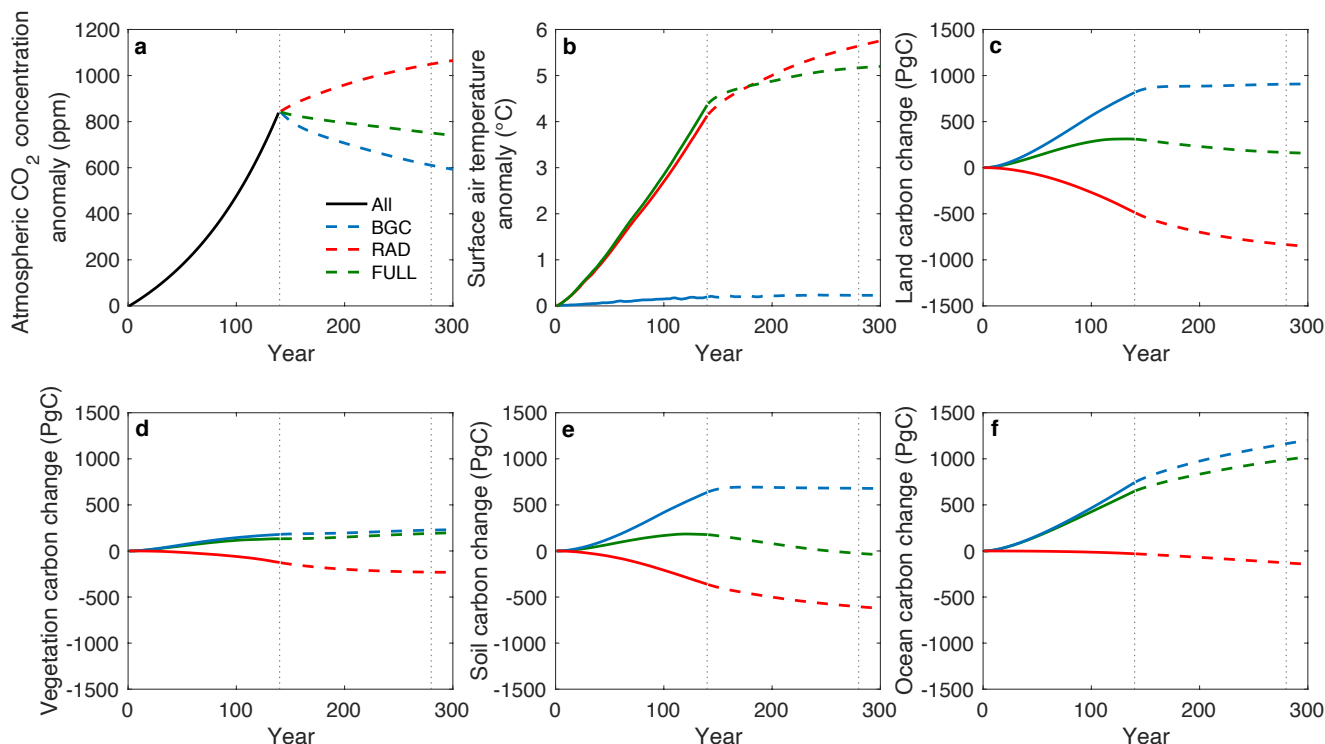


### 3.2 Improving the Quantification of Carbon Cycle Feedbacks under Negative Emissions

#### 330 3.2.1 “Zeroemit” Simulation: Quantifying Climate System Inertia

Zero emissions simulations quantify committed changes due to prior positive emissions. Changes in atmospheric CO<sub>2</sub> concentration in zero emissions simulations are driven by the carbon sinks, which in turn are influenced by the CO<sub>2</sub> concentration and climate. Following cessation of emissions, the CO<sub>2</sub> concentration in the FULL mode declines steadily, mainly driven by ocean carbon uptake consistent with results from MacDougall et al. (2020) (**figure 7(a)**). The CO<sub>2</sub> concentration in the BGC mode declines more than in the FULL mode because both land and ocean remain carbon sinks. In the RAD mode, the CO<sub>2</sub> concentration increases as both land and ocean release CO<sub>2</sub> into the atmosphere. Changes in atmospheric CO<sub>2</sub> concentration, together with changes in ocean heat uptake and surface albedo, drive changes in surface air temperature. In the FULL mode, the warming effect of declining ocean heat uptake dominates over the cooling effect of declining CO<sub>2</sub> concentration resulting in continued warming (MacDougall et al., 2020) (**figure 7(b); figure S6**). Surface air temperature in the RAD mode increases more than in the FULL mode because the CO<sub>2</sub> concentration increases, causing further warming. Surface air temperature remains relatively constant in the BGC mode. In the FULL mode, the land switches into a source of carbon after emissions cease, consistent with the behaviour of the UVic ESCM in the Zero Emissions Commitment Model Intercomparison Project (ZECMIP) (MacDougall et al., 2020) (**figure 7(c)**). The vegetation carbon pool continues to take up carbon (**figure 7(d)**) whereas, the soil switches into a source of carbon (**figure 7(e)**). The ocean remains a carbon sink after cessation of emissions (**figure 7(f)**). In the BGC mode, the ocean remains a strong carbon sink after CO<sub>2</sub> emissions are set to zero, whereas the land initially takes up carbon, stabilizes, then becomes a weak carbon sink again (**figure 7(c, f)**). The vegetation carbon pool takes up carbon throughout the zero emissions phase whereas, the soil initially takes up carbon, stabilizes, then slowly releases CO<sub>2</sub> (**figure 7(d, e)**). Both land and ocean release CO<sub>2</sub> to the atmosphere in the RAD mode (**figure 7(c, f)**) with both vegetation and soil carbon pools driving the land carbon release (**figure 7(d, e)**).

350



355 **Figure 7:** a. Atmospheric CO<sub>2</sub> concentration anomaly b. surface air temperature change c. land carbon change d. vegetation carbon change f. soil carbon change and d. ocean carbon change for the zero emissions simulations relative to 1850 (preindustrial). BGC = biogeochemically coupled, RAD = radiatively coupled and FULL = fully coupled. Solid lines are for the ramp-up phase; dashed lines are for the zero emissions phase.

### 3.2.2 “Ramp-down – Zeroemit” Approach: Isolating the Response to Negative Emissions

The “Ramp-down – Zeroemit” approach uses the zero emissions simulations described in the previous section to isolate the response to negative emissions in the “CDR-reversibility” simulations by taking the difference between the ramp-down phase of the RAD (BGC) “CDR-reversibility” simulation and the RAD (BGC) zero emissions simulation. In the BGC mode, despite our attempt to reduce climate system inertia in our novel approach, carbon pools do not return to their preindustrial states at the time atmospheric CO<sub>2</sub> returns to preindustrial levels (**figure 5**). In the RAD mode, all carbon pools gain more carbon than they held at preindustrial (**figure 6**).

The “Ramp-down – Zeroemit” approach removes the initial carbon increase (decrease) in the “CDR-reversibility” BGC (RAD) mode, reducing the width of the hysteresis (**figure 6**). Zickfeld et al. (2016) used zero emissions to isolate the response to negative emissions and observed a reduction in the initial carbon change at the beginning of the ramp-down phase consistent with our results. One possible reason why the hysteresis persists may be irreversible changes in vegetation distribution in the “CDR-reversibility” ramp-down phase that are caused by state changes rather than inertia. Alternatively, the hysteresis may





370 show that the linearity assumption made in this experiment, that is, the assumption that the committed carbon cycle response to past positive emissions and the carbon cycle response to negative emissions combine linearly to the total carbon cycle response in the ramp-down phase in this experimental design, is not satisfied.

375 Isolating the response to negative emissions alone in the “Ramp-down – Zeroemit” approach, the magnitudes of  $\beta_L$  and  $\beta_O$  are smaller under negative emissions as compared to their respective magnitudes under positive emissions, but the magnitudes of  $\gamma_L$  and  $\gamma_O$  become larger under negative emissions (**Table 1**). Under negative emissions, the magnitudes of  $\beta$  and  $\gamma$  from our novel approach are larger compared to those from the “CDR-reversibility” simulation, implying greater carbon loss due to the concentration-carbon feedback and greater carbon gain due to the climate-carbon feedback under negative emissions. For example, a decrease in atmospheric CO<sub>2</sub> of one ppm would result in the loss of 0.68 PgC of land carbon in the standard approach and 0.80 PgC of land carbon in our approach due to the concentration-carbon feedback whereas, cooling by one  
380 degree, would result in land carbon gain of 56.4 PgC in the standard approach and almost three times as much (157.1 PgC) in our approach due to the climate-carbon feedback.

#### 4 Discussion and conclusions

Our results from the “CDR-reversibility” simulation show that, due to the concentration-carbon feedback, carbon pools take up carbon in the ramp-up phase, continue to take up carbon in the early ramp-down phase, then switch into sources of carbon.  
385 Due to the climate-carbon feedback, carbon pools lose carbon in the ramp-up phase, continue to lose carbon in the ramp-down phase, then switch into carbon sinks. Furthermore, the land and ocean carbon pools do not return to their preindustrial states at the end of both modes, suggesting that land and ocean carbon changes due to carbon cycle feedbacks in the ramp-up phase are irreversible on centennial timescales. The differences in the magnitudes of carbon cycle feedbacks in the ramp-up and ramp-down phases, as quantified by feedback parameters, are likely largely due to climate system inertia. This inertia reduces the magnitude of both feedbacks under negative emissions relative to feedbacks under positive emissions, implying reduced  
390 carbon loss due to the concentration-carbon feedback and reduced carbon gain due to the climate-carbon feedback.

To quantify the carbon cycle inertia, that is, the response to prior positive emissions, we ran zero emissions simulations in fully coupled, biogeochemically coupled and radiatively coupled modes. Consistent with previous studies, the ocean continues to sequester carbon in the fully coupled zero emissions simulation (MacDougall et al., 2020). The terrestrial biosphere switches  
395 into a carbon source after emissions cease, consistent with the behaviour of the UVic ESCM in the Zero Emissions Commitment Model Intercomparison Project (ZECMIP) (MacDougall et al., 2020). Carbon uptake, largely by the ocean sink, decreases the atmospheric CO<sub>2</sub> concentration. Surface air temperature increases due to the interplay between declining CO<sub>2</sub> concentration and ocean heat uptake (Matthews & Caldeira, 2008; Solomon et al., 2009; Arora et al., 2013). The carbon pools  
400 in the biogeochemically coupled and radiative coupled zero emissions simulations also exhibit inertia: the land and ocean



continue to sequester carbon after cessation of emissions in the biogeochemically coupled simulation, whereas both carbon pools release CO<sub>2</sub> in the radiatively coupled simulation.

405 Assuming linearity in the response to prior positive emissions and negative emissions, we subtract the zero emissions simulations from the “CDR-reversibility” simulations, to isolate the response to negative emissions alone. We find that under negative emissions, the magnitudes of  $\beta$  and  $\gamma$  from our novel approach are larger as compared to those from the “CDR-reversibility” simulation, implying greater carbon loss and carbon gain due to the concentration-carbon and climate-carbon feedbacks respectively if feedback parameters from our approach are applied instead. Furthermore, land and ocean carbon changes in the ramp-up phase remain irreversible in our approach.

410 A similar feedback analysis was conducted for ocean carbon cycle feedbacks using the Norwegian Earth System Model (NorESM) (Schwinger & Tjiputra, 2018). Schwinger and Tjiputra calculated ocean concentration-carbon and climate-carbon feedback parameters using the same carbon cycle feedback framework and “CDR-reversibility” simulations used here. Their results also show a lagged ocean carbon response to positive emissions in the ramp-down phase, and as a result, the magnitude of both carbon cycle feedbacks is smaller under negative missions than under positive emissions.

We compare carbon cycle feedback parameters under positive emissions quantified from the “CDR-reversibility” simulation to model means and standard deviations from CMIP5 and CMIP6 – the fifth and sixth phases of the Coupled Model Intercomparison Project – respectively (Arora et al., 2020) (see **supplementary table 2**). The concentration-carbon feedback parameter for land ( $\beta_L$ ) is generally consistent with those from CMIP5 and CMIP6, while the ocean concentration-carbon feedback parameter ( $\beta_O$ ) lies slightly above the CMIP6 range. The land climate-carbon feedback parameter ( $\gamma_L$ ) lies well above the CMIP5 and CMIP6 ranges, implying a stronger sensitivity to warming relative to CMIP5 and CMIP6 models. The ocean climate-carbon feedback parameter ( $\gamma_O$ ) is consistent with those from CMIP5 and CMIP6.

425 The version of the UVic ESCM used here does not represent the nitrogen cycle on land and its coupling to the carbon cycle, which has ramifications for the estimated magnitude of carbon cycle feedbacks. Models without a nitrogen cycle exhibit greater land carbon gain under positive emissions relative to other CMIP5 and CMIP6 models, that is, the concentration-carbon feedback parameter is more positive (**Table S2**). They also exhibit greater carbon loss under positive emissions, that is, the climate-carbon feedback parameter is more negative. Therefore, the magnitude of both carbon cycle feedbacks in this study is generally larger under positive emissions relative to other CMIP5 and CMIP6 models with a nitrogen cycle. Due to the exclusion of the nitrogen cycle, the UVic ESCM is expected to exhibit smaller carbon losses due to the concentration-carbon feedback and greater carbon gain due to the climate-carbon feedback under negative emissions relative to CMIP5 and CMIP6 models with a nitrogen cycle. With the consideration of nitrogen limitation, the already weakened CO<sub>2</sub> fertilization effect



under declining CO<sub>2</sub> concentrations would be further constrained, exacerbating the carbon loss due to the concentration-carbon  
435 feedback. On the contrary, nitrogen remineralization would decline as surface air temperature declines, reducing the carbon  
gain due to the climate-carbon feedback.

Each of the two approaches used here to quantify carbon cycle feedback parameters has its benefits and drawbacks. Because  
the “CDR-reversibility” simulation is commonly used in literature (Schwinger & Tjiputra, 2018; Keller et al., 2018; Zickfeld  
440 et al., 2016), it allows easier comparison of results across models. However, research shows that this idealized scenario may  
delay the land sink-to-source transition, and underestimate ocean carbon uptake and the strength of the permafrost carbon  
feedback (MacDougall, 2019). The main limitation is that carbon cycle feedback parameters quantified for the ramp-down  
phase include carbon cycle inertia effects, making this approach inaccurate for quantifying carbon cycle feedbacks under  
negative emissions.

445  
In their 2016 paper, Zickfeld et al. used zero emissions simulations to correct for the thermal and carbon cycle inertia in a suite  
of “CDR-reversibility” simulations, similar to our novel approach in this study. This reduced, but did not eliminate the climate  
system inertia, consistent with our results. Although our approach does not eliminate the inertia, it provides a more accurate  
estimate of the magnitude of carbon cycle feedbacks under negative emissions by reducing the response to prior positive  
450 emissions, bringing the estimate closer to a quantification of carbon cycle feedbacks under negative emissions alone. We  
hypothesize that the remaining inertia may be related to irreversible changes in vegetation distribution in the “CDR-  
reversibility” simulations. Alternatively, the linearity assumption made in this experimental design may not hold. If the  
responses to prior positive emissions and negative emissions are not additive, then the zero emissions simulations may not  
quantify and remove all the inertia in the “CDR-reversibility” simulations. Lastly, the remaining inertia may be associated  
455 with the different configurations in which the “CDR-reversibility” and “Zeroemit” simulations were run: the former were run  
in concentration-driven mode whereas, the latter were emissions-driven. Therefore, changes in land and ocean carbon fluxes  
affect the atmospheric CO<sub>2</sub> concentration in the zero emissions simulations, but not in the “CDR-reversibility” simulations.

Carbon cycle feedbacks under negative emissions are currently quantified from the ramp-down phase of the “CDR-  
460 reversibility” simulation. However, this approach underestimates the magnitudes of carbon cycle feedbacks because the  
response in the ramp-down phase includes climate system inertia effects that weaken both feedbacks. Our novel approach aims  
to reduce the inertia in the ramp-down phase, thereby improving the quantification of carbon cycle feedbacks under negative  
emissions. We find that the magnitudes of the concentration-carbon and climate-carbon feedbacks under negative emissions  
are larger in our approach as compared to the standard approach. This has two implications: using feedback parameters from  
465 the standard approach will (1) underestimate carbon release under negative emissions due to the concentration-carbon  
feedback, and (2) underestimate carbon gain due to the climate-carbon feedback. Given that the concentration-carbon feedback  
is the dominant feedback, quantifying carbon cycle feedbacks under negative emissions from the “CDR-reversibility”



simulation will result in the underestimation of carbon loss under negative emissions, thereby overestimating the effectiveness of negative emissions in drawing down CO<sub>2</sub>.

470

Future research should test the robustness of these results in a multi-model framework. A first step could be analyzing the “CDR-reversibility” simulations in three modes (biogeochemically coupled, radiatively coupled and fully coupled) in the next CMIP phase. In addition, positive and negative CO<sub>2</sub> emissions could be applied from an equilibrium state to overcome issues related to climate system inertia.

#### 475 **5 Code/Data Availability**

The UVic ESCM data will be made available after publishing and the model code for UVic ESCM 2.10 is available at <http://terra.seos.uvic.ca/model/2.10/>.

#### **6 Author contribution**

480 K.Z. developed the research question and worked with C.N. on the initial data analysis. V.R.C ran the model simulations and worked with K.Z. to analyse and interpret the model data and write the manuscript. C.N. also helped revise the manuscript.

#### **7 Competing interests**

The authors declare no competing interests.

#### **8 Acknowledgements**

485 This research was funded by the Natural Sciences and Engineering Research Council (NSERC) Discovery Grant Program. Computing resources were provided by the Digital Research Alliance of Canada (formerly Compute Canada).

#### **References**

- Arora, V. K., Boer, G. J., Friedlingstein, P., Eby, M., Jones, C. D., Christian, J. R., Bonan, G., Bopp, L., Brovkin, V., Cadule, P., Hajima, T., Ilyina, T., Lindsay, K., Tjiputra, J. F., and Wu, T.: Carbon–Concentration and Carbon–Climate Feedbacks in CMIP5 Earth System Models, *J. Climate*, 26, 5289–5314, <https://doi.org/10.1175/JCLI-D-12-00494.1>, 2013.
- 490 Arora, V. K., Katavouta, A., Williams, R. G., Jones, C. D., Brovkin, V., Friedlingstein, P., Schwinger, J., Bopp, L., Boucher, O., Cadule, P., Chamberlain, M. A., Christian, J. R., Delire, C., Fisher, R. A., Hajima, T., Ilyina, T., Joetzjer, E., Kawamiya, M., Koven, C., Krasting, J., Law, R. M., Lawrence, D. M., Lenton, A., Lindsay, K., Pongratz, J., Raddatz, T., Séférian, R., Tachiiri, K., Tjiputra, J. F., Wiltshire, A., Wu, T., and Ziehn, T.: Carbon-concentration and carbon-climate feedbacks in



- 495 CMIP6 models, and their comparison to CMIP5 models, *Biogeosciences*, 17, 4173–4222, doi.org/10.5194/bg-17-4173-2020, 2020.
- Boer, G. J. & Arora, V.: Geographic Aspects of Temperature and Concentration Feedbacks in the Carbon Budget, *J. Clim.*, 23(3), 775–784, doi: 10.1175/2009JCLI3161.1, 2010.
- Boer, G. J. & Arora, V.: Feedbacks in emission-driven and concentration-driven global carbon budgets, *J. Clim.*, 32(10), 3326–3341, doi: 10.1175/JCLI-D-12-00365.1, 2013.
- 500 Boucher, O., Halloran, P. R., Burke, E. J., Doutriaux-Boucher, M., Jones, C. D., Lowe, J., Ringer, M. A., Robertson, E., and Wu, P.: Reversibility in an earth system model in response to CO<sub>2</sub> concentration changes, *Environ. Res. Lett.*, 7, 024013, doi: 10.1088/1748-9326/7/2/024013, 2012.
- Cao, L. & Caldeira, K.: Atmospheric carbon dioxide removal: Long term consequences and commitment, *Environ. Res. Lett.*, 5, 024011, doi: 10.1088/1748-9326/5/2/024011, 2010.
- 505 Ciais, P., Sabine, C., Bala, G., Bopp, L., Brovkin, V., Canadell, J., Chhabra, A., DeFries, R., Galloway, J., Heimann, M., Jones, C., Le Quéré, C., Myneni, R. B., Piao, S. and Thornton, P.: Carbon and Other Biogeochemical Cycles, in: Working Group I Contribution to the Intergovernmental Panel on Climate Change Fifth Assessment Report Climate Change 2013: The Physical Science Basis, edited by: Stocker, T. F., Qin, D., Plattner, G.-K., Tignor, M., Allen, S. K., Boschung, J., Nauels, A., Xia, Y., Bex, V., and Midgley, P., Cambridge University Press, 2013.
- 510 Cox, P. M., Betts, R. A., Jones, C. D., Spall, S. A., & Totterdell, I.: Acceleration of global warming due to carbon-cycle feedbacks in a coupled climate model, *Nature*, 408, 184–187, doi: 10.1038/35041539, 2000.
- Cox, P.: Description of the TRIFFID Dynamic Global Vegetation Model, Hadley Centre Technical Note # 24, UK Met Office, available at: [https://digital.nmla.metoffice.gov.uk/IO\\_cc8f146a-d524-4243-88fc-e3a3bcd782e7/](https://digital.nmla.metoffice.gov.uk/IO_cc8f146a-d524-4243-88fc-e3a3bcd782e7/) (last access: June 2022), 2001
- 515 Eby, M., Weaver, A. J., Alexander, K., Zickfeld, K., Abe-Ouchi, A., Cimadoribus, A., Cresspin, E., Drijfhout, S. S., Edwards, N. R., Eliseev, A. V., Feulner, G., Fichefet, T., Forest, C. E., Goose, H., Holden, P. B., Joos, F., Kawamiya, M., Kicklighter, D., Kienert, H., Matsumoto, K., Mokhov, I. I., Monier, E., Olsen, S. M., Pedersen, J. O. P., Perrette, M., Philippon-Berthier, G., Ridgwell, A., Schlosser, A., Schneider von Deimling, T., Shaffer, G., Smith, R. S., Spahni, R., Sokolov, A. P., Steinacher, M., Tachiiri, K., Tokos, K., Yoshimiri, M., Zeng, N., and Zhao, F.: Historical and idealized climate model
- 520 experiments: An intercomparison of Earth system models of intermediate complexity, *Clim. Past*, 9(3), 1111–1140, doi:10.5194/cp-9-1111-2013, 2013.
- Eyring, V., Bony, S., Meehl, G. A., Senior, C. A., Stevens, B., Stouffer, R. J., and Taylor, K. E.: Overview of the Coupled Model Intercomparison Project Phase 6 (CMIP6) experimental design and organization, *Geosci. Model Dev.*, 9, 1937–1958, doi.org/10.5194/gmd-9-1937-2016, 2016.
- 525 Friedlingstein, P., Cox, P., Betts, R., Bopp, L., Von Bloh, W., Brovkin, V., Cadule, P., Doney, S., Eby, M., Fung, I., Bala, G., John, J., Jones, C., Joos, F., Kato, T., Kawamiya, M., Knorr, W., Lindsay, K., Matthews, H. D., Raddatz, T., Rayner, P., Reick, C., Roeckner, E., Schnitzler, K.-G., Schnur, R., Strassmann, K., Weaver, A. J., Yoshikawa, C., Zeng, A. N., and Friedlingstein, P.: Climate–Carbon Cycle Feedback Analysis: Results from the C4 MIP Model Intercomparison, *J. Clim.*, 19, 3337–3353, doi.org/10.1175/JCLI3800.1, 2006.
- 530 Friedlingstein, P., Jones M. W., O’Sullivan, M., Andrew, R. M., Bakker, D. C. E., Hauck, J., Le Quéré, C., Peters, G. P., Peters, W., Pongratz, J., Sitch, S., Canadell, J. G., Ciais, P., Jackson, R. B., Alin, S. R., Anthoni, P., Bates, N. R., Becker, M., Bellouin, N., Bopp, L., Chau, T. T. T., Chevallier, F., Chini, L. P., Cronin, M., Currie, K. I., Decharme, B., Djeutchouang, L. M., Dou, X., Evans, W., Feely, R. A., Feng, L., Gasser, T., Gilfillan, D., Gkritzalis, T., Grassi, G., Gregor, L., Gruber, N., Gürses, O., Harris, I., Houghton, R. A., Hurtt, G. C., Iida, Y., Ilyina, T., Luijkx, I. T., Jain, A., Jones, S. D., Kato, E.,
- 535 Kennedy, D., Goldewijk, K. K., Knauer, J., Korsbakken, J. I., Körtzinger, A., Landschützer, P., Lauvset, S. K., Lefèvre, N., Lienert, S., Liu, J., Marland, G., McGuire, P. C., Melton, J. R., Munro, D. R., Nabel, J. E. M. S., Nakaoka, S., Niwa, Y., Ono, T., Pierrot, D., Poulter, B., Rehder, G., Resplandy, L., Robertson, E., Rödenbeck, C., Rosan, T. M., Schwinger, J., Schwingshackl, C., Séférian, R., Sutton, A. J., Sweeney, C., Tanhua, T., Tans, P. P., Tian, H., Tillbrook, B., Tubiello, F., van der Werf, G. R., Vuichard, N., Wada, C., Wanninkhof, R., Watson, A. J., Willis, D., Witshire, A. J., Yuan, W., Yue, C., Yue,



- 540 X., Zaehle, S., and Zeng, J.: Global Carbon Budget 2021, *Earth. Syst. Sci. Data*, 14, 1917 – 2005, doi: 10.5194/essd-14-1917-2022, 2022.
- Friedlingstein, P., Meinshausen, M., Arora, V., Jones, C., Anav, A., Liddicoat, S., & Knutti, R.: Uncertainties in CMIP5 climate projections due to carbon cycle feedbacks, *J. Clim.*, 27(2), 511–526, doi: 10.1175/JCLI-D-12-00579.1, 2014.
- Fung, I.Y., Doney, S. C., Lindsay, K., & Jasmin J. G.: Evolution of carbon sinks in a changing climate, *PNAS*, 102(32), 11201–11206, doi: 10.1073/pnas.0504949102, 2005.
- 545 Fuss, S., Canadell, J. G., Peters, G. P., Tavoni, M., Andrew, R. M. Ciais, P., Jackson, R. B., Jones, C. D., Kraxner, F., Nakicenovic, N., Le Quéré, C., Raupach, M. R., Sharifi, A., Smith P., and Yamagata, Y.: Betting on negative emissions, *Nat. Clim. Change*, 1–3, doi.org/10.1038/nclimate2392, 2014.
- IPCC.: *Climate Change 2022: Impacts, Adaptation, and Vulnerability, Contribution of Working Group II to the Sixth Assessment Report of the Intergovernmental Panel on Climate Change* [H.-O. Pörtner, D.C. Roberts, M. Tignor, E.S. Poloczanska, K. Mintenbeck, A. Alegría, M. Craig, S. Langsdorf, S. Löschke, V. Möller, A. Okem, B. Rama (eds.)], Cambridge University Press, In Press, 2022.
- 550 Jones, C. D., Arora, V., Friedlingstein, P., Bopp, L., Brovkin, V., Dunne, J., Graven, H., Hoffman, F., Ilyina, T., John, J. G., Jung, M., Kawamiya, M., Koven, C., Pongratz, J., Raddatz, T., Randerson, J. T., and Zaehle, S.: C4MIP – The Coupled Climate-Carbon Cycle Model Intercomparison Project: experimental protocol for CMIP6, *Geosci. Model Dev.*, 9, 2853–2880, doi: 10.5194/gmd-9-2853-2016, 2016.
- 555 Jones, C. D., Ciais, J., Davis, S. J., Friedlingstein, P., Gasser, T., Peters, G. P. ... Wiltshire, A.: Simulating the Earth System response to negative emissions, *Environ. Res. Lett.*, 11, 095012, doi: 10.1088/1748-9326/11/9/095012, 2016.
- Jones, C. D., Cox, P. M., Essery, R. L. H., Roberts, D. L., and Woodage, M. J.: Strong carbon cycle feedbacks in a climate model with interactive CO<sub>2</sub> and sulphate aerosols, *Geophys. Res. Lett.*, 30(9), 1479, doi:10.1029/2003GL016867, 2003.
- 560 Keller, D. P., Lenton, A., Scott, V., Vaughan, N. E., Bauer, N., Ji, D. ... Zickfeld, K.: The Carbon Dioxide Removal Model Intercomparison Project (CDRMIP): Rationale and experimental protocol for CMIP6, *Geosci. Model Dev.*, 11, 1133 – 1160, doi: 10.5194/gmd-11-1133-2018, 2018.
- Keller, D. P., Oschlies, A. & Eby, M.: A new marine ecosystem model for the University of Victoria earth system climate model, *Geosci. Model Dev.*, 5(5), 1195–1220, doi: 10.5194/gmd-5-1195-2012, 2012.
- 565 MacDougall, A. H.: Limitations of the 1 % experiment as the benchmark idealized experiment for carbon cycle intercomparison in C4MIP, *Geosci. Model Dev.*, 12, 597–611, doi: 10.5194/gmd-12-597-2019, 2019.
- MacDougall, A. H. & Knutti, R.: Projecting the release of carbon from permafrost soils using a perturbed parameter ensemble modelling approach, *Biogeosciences*, 13, 2123–2136, doi: 10.5194/bg-13-2123-2016, 2016.
- 570 MacDougall, A. H., Frölicher, T. L., Jones, C. D., Rogelj, J., Matthews, H. D., Zickfeld, K., Arora, V. K., Barrett, N. J., Brovkin, V., Burger, F. A., Eby, M., Eliseev, A. V., Hajima, T., Holden, P. B., Jeltsch-Thömmes, A., Koven, C., Mengis, N., Menviel, L., Michou, M., Mokhov, I. I., Oka, A., Scwinger, J., Séférian, R., Shaffer, G., Sokolov, A., Tachiiri, K., Tjiputra, J., Wiltshire, A. and Ziehn, T.: Is there warming in the pipeline? A multi-model analysis of zero emissions commitment of CO<sub>2</sub>, *Biogeosciences*, 17, 2987–3016, doi: 10.5194/bg-17-2987-2020, 2020.
- 575 Matthews, H. D. and Caldeira, K.: Stabilizing climate requires near-zero emissions, *Geophys. Res. Lett.*, 35, L04705, doi: 10.1029/2007GL032388, 2008.
- Meissner, K. J., Weaver, A. J., Matthews, H. D. & Cox, P. M.: The role of land surface dynamics in glacial inception: a study with the UVic Earth System Model, *Clim. Dyn.*, 21(7–8), 515–537, doi: 10.1007/s00382-003-0352-2. 2003.
- 580 Mengis, N., Keller, D. P., MacDougall, A., Eby, M., Wright, N., Meissner, K. J. Oschlies, A., Schmittner, A., MacIsaac, A. J., Matthews, H. D., and Zickfeld, K.: Evaluation of the University of Victoria Earth System Climate Model version 2.10 (UVic ESCM 2.10), *Geosci. Model Dev. Discuss.*, 1–28, doi: 10.5194/gmd-13-4183-2020, 2020.
- Pacanowski, R. C.: MOM 2 Documentation, users guide and reference manual, GFDL Ocean Group Technical Report 3, Geophys. Fluid Dyn. Lab., Princet. Univ. Princeton, NJ, 1995.
- Park, S. & Kug, J.: Hysteresis of terrestrial carbon cycle to CO<sub>2</sub> ramp-up and -down forcing, PREPRINT (Version 1)
- 585 available at Research Square, doi: 10.21203/rs.3.rs-1074581/v1, 2021.





- Rogelj, J., Forster, P. M., Kriegler, E., Smith, C. J., and Séférian, R.: Estimating and tracking the remaining carbon budget for stringent climate targets, *Nature*, 571, 335–342, doi: 10.1038/s41586-019-1368-z, 2019.
- Rogelj, J., Shindell, D., Jiang, K., Fifita, S., Forster, P., Ginzburg, V., Handa, C., Kheshgi, H., Kobayashi, S., Kriegler, E., Mundaca, L., Seferian, R., and Vilarino, M. V.: Mitigation Pathways Compatible with 1.5 °C in the Context of Sustainable Development, in: *Global Warming of 1.5 °C. An IPCC Special Report on the impacts of global warming of 1.5 °C above pre-industrial levels and related global greenhouse gas emission pathways, in the context of strengthening the global response to the threat of climate change, sustainable development, and efforts to eradicate poverty*, edited by: Masson-Delmotte, V., Zhai, P., Pörtner, H.-O., Roberts, D., Skea, J., Shukla, P. R., Pirani, A., Moufouma-Okia, W., Péan, C., Pidcock, R., Connors, S., Matthews, J. B. R., Chen, Y., Zhou, X., Gomis, M. I., Lonnoy, E., Maycock, T., Tignor, M., and Waterfield, T., available at: <https://www.ipcc.ch/report/sr15/mitigation-pathways-compatible-with-1-5c-in-the-context-of-sustainable-4-development/>, 2018.
- Schwinger, J. and Tjiputra, J.: Ocean Carbon Cycle Feedbacks Under Negative Emissions, *Geophys. Res. Lett.*, 45, 5062–5070, doi: 10.1029/2018GL077790, 2018
- Solomon, S., Plattner, G.-K., Knutti, R., and Friedlingstein, P.: Irreversible climate change due to carbon dioxide emissions, *P. Natl. Acad. Sci.*, 106, 1704–1709, doi: 10.1073/pnas.0812721106, 2009.
- Tokarska, K. B. & Zickfeld, K.: The effectiveness of net negative carbon dioxide emissions in reversing anthropogenic climate change, *Environ. Res. Lett.*, 094013, doi: 10.1088/1748-9326/10/9/094013, 2015.
- UNFCCC.: Adoption of the Paris Agreement. Retrieved from <https://unfccc.int/sites/default/files/resource/docs/2015/cop21/eng/109r01.pdf>, 2022.
- Weaver, A. J., Eby, M., Wiebe, E. C., Bitz, C. M., Duffy, P. B., Ewen, T. L., ... Fanning, A. F.: The UVic Earth System Climate Model: Model description, climatology, and applications to past, present and future climates, *Atmosphere Ocean*, 39, 361-428, 2001.
- Zickfeld, K., Azevedo, D., Mathesius, S. & Matthews, H. D.: Asymmetry in the climate–carbon cycle response to positive and negative CO<sub>2</sub> emissions, *Nat. Clim. Chang.* 11, 613–617, doi: 10.1038/s41558-021-01061-2, 2021.
- Zickfeld, K., Eby, M., Matthews, H. D., Schmittner, A., and Weaver, A. J.: Nonlinearity of Carbon Cycle Feedbacks, *J. Climate*, 24, 4255–4275, doi: 10.1175/2011JCLI3898.1, 2011.
- Zickfeld, K., MacDougall, A. H., & Matthews, H. D.: On the proportionality between global temperature change and cumulative CO<sub>2</sub> emissions during periods of net negative CO<sub>2</sub> emissions, *Environ. Res. Lett.*, 11(5), 055006, doi: 10.1088/1748-9326/11/5/055006, 2016.
- Ziehn, T., Lenton, A. & Law, R.: An assessment of land-based climate and carbon reversibility in the Australian Community Climate and Earth System Simulator, *Mitig. Adapt. Strateg. Glob. Change*, 25, 713–731, doi: 10.1007/s11027-019-09905-1, 2020.